

Non-linear waves with electromagnetic interaction in aluminium electrolysis cells

V.Bojarevics*

*University of Greenwich, School of Computing and Mathematics
Wellington Str., London SE18 6PF, UK*

Introduction

An aluminum electrolytic cell contains two overlying fluid layers of small density difference and large horizontal extent relative to their depth. The interface waves are similar to stratified sea layers, but the situation is complicated by the passage of electric current exceeding in modern cells a magnitude of 200,000 A. The interface waves change electric current distribution in accordance to depth variation of poorly conducting electrolyte what produces high density horizontal currents in the relatively thin and well conducting liquid aluminium. The wave development depends on the magnetic field distribution created by the current supplying busbars and by the current in the cell. The interface stability problem is of great practical importance because the electrolytic aluminium production is a major electrical energy consumer, and it is related to environmental pollution rate.

Urata et al.¹ were the first to introduce a coupled wave equation to describe the interface evolution in electrolysis cells. In their model the electric current is coupled to the interface deformation. In Ref.² a systematic perturbation expansion is developed for the fluid dynamics and electric current problems which permitted to reduce the three-dimensional problem to a two-dimensional one for the leading order expansion terms.

The procedure is more generally known as “shallow water approximation” which can be extended for the case of weakly non-linear and dispersive waves. Generalised KdV equation was derived by Hofman³ for small finite amplitude gravity waves in the presence of magnetic field. Oshima and Yamane⁴ applied numerical analysis of the generalised Boussinesq equations to investigate unidirectional propagation of a solitary wave and a hydraulic bore, and obtained qualitative agreement to their experimental results. The Boussinesq formulation permits to generalise problem for non-unidirectionally propagating waves, accounting for side walls and for a two fluid layer

* Senior Research Fellow

Paper presented at the 8th Beer-Sheva International Seminar on “MHD Flows and Turbulence”, Jerusalem, February 1996.

interface, e.g., Renouard et al.⁵ found a good correspondence to the experimental results for resonantly interacting waves in a channel mounted on a rotating platform.

In the present work shallow layer generalised Boussinesq equations are derived for wave motions depending on two horizontal variables x, y for two layers and with the electromagnetic interaction which makes the flow velocities rotational. Thus the velocity potential alone will not be adequate for the flow representation. The mathematical problem is put in “weak” formulation and coupled equations in Fourier space are derived. The solution method is a discrete time stepping where the full non-linear problem is linearized within each small time step and the resulting eigenvalue/eigenvector problem solved numerically by high accuracy LAPACK routines. The procedure can be considered as an extension of the linear stability problem. The simulated wave behavior will be validated against the one-dimensional finite amplitude standing wave analytical solutions by Tadjbakhsh and Keller⁶. Different magnetically modified wave patterns will be presented graphically.

Statement of the problem

An idealised electrolysis cell can be represented by three layers shown in Fig.1 where the top layer (3) is solid carbon anode, (2) - liquid electrolyte of density $\rho_2=2.1 \cdot 10^3 \text{ kg/m}^3$ and (3) molten aluminium - $\rho_1=2.3 \cdot 10^3 \text{ kg/m}^3$. The horizontal dimensions L_x and L_y are assumed to be much larger than the typical depth H and the interface wave typical amplitude A is assumed to be small relative to the depth. Thus two small parameters of the problem are

$$\delta = \frac{H}{L} \ll 1$$

$$\varepsilon = \frac{A}{H} \ll 1$$

and they are assumed to be related as $\varepsilon = O(\delta^2)$.

With the purpose to derive weakly nonlinear shallow layer approximation Boussinesq equations we will need to estimate the terms in the full equations of motion. Therefore, nondimensional variables are introduced using the following scales: L for coordinates x, y ; $\varepsilon \sqrt{gH}$ for velocity \mathbf{v} , L/\sqrt{gH} for time t , $\rho_1 gH$ for pressure p , IB_0/L^2 for electromagnetic force \mathbf{f} (B_0 is typical magnetic field magnitude and I - total electric current). According to the small depth assumption a stretched nondimensional coordinate $\bar{z} = z/(L\delta)$ is defined, and the nondimensional interface deformation is represented as $\bar{h}_o = \varepsilon \zeta(x, y, t)$. With these definitions the nondimensional fluid flow equations: continuity, horizontal momentum and vertical momentum transport, are respectively,

$$\partial_k u_k + \delta^{-1} \partial_{\bar{z}} w = 0 \quad (1)$$

$$\begin{aligned} \partial_t u_j + \varepsilon \partial_k (u_k u_j) + \varepsilon \delta^{-1} \partial_{\bar{z}} (u_j w) = \\ - \varepsilon^{-1} \partial_j p + \text{Re}^{-1} (\varepsilon \delta^{-2} \partial_{\bar{z}\bar{z}} u_j + \varepsilon \partial_{kk} u_j) + E f_j \end{aligned} \quad (2)$$

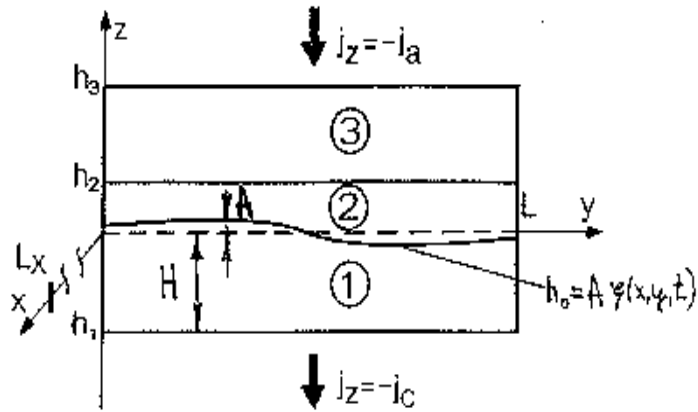


Fig. 1 Idealized electrolysis cell.

$$\begin{aligned} \partial_t w + \varepsilon \partial_k (u_k w) + \varepsilon \delta^{-1} \partial_z w^2 = \\ = -\varepsilon^{-1} \delta^{-1} \partial_z p + \text{Re}^{-1} (\varepsilon \delta^{-2} \partial_{\bar{z}} w + \varepsilon \partial_{kk} w) + E f_z - \varepsilon^{-1} \delta^{-1} \end{aligned} \quad (3)$$

where Einstein summation convention is assumed over the repeating j and k indexes (equal to 1 or 2, respectively for x, y coordinates) is used, and the nondimensional governing parameters are Reynolds number:

$$\text{Re} = \frac{L\varepsilon\sqrt{gH}}{\nu} \quad \text{and electromagnetic interaction parameter: } E = \frac{IB_o}{L^2\rho g\varepsilon\delta}.$$

Formally the Boussinesq equations can be derived if assuming $\text{Re}^{-1}\varepsilon\delta^{-2} = O(1)$ and $E = O(1)$, and the leading terms of velocity expansion in the small depth parameter being given by

$$\mathbf{u}(x, y, z, t) = \mathbf{u}_o(x, y, t) + \delta \mathbf{u}_\delta(x, y, z, t) + o(\delta). \quad (4)$$

The continuity equation (1) shows that the vertical velocity expansion starts with the second term only:

$$w(x, y, z, t) = \delta w_\delta + o(\delta). \quad (5)$$

Depth averaged quantities are introduced according to the definition:

$$\bar{u}_j(x, y, t) = \frac{1}{h_i - h_o} \int_{h_o}^{\bar{h}_i} u_j d\bar{z}. \quad (6)$$

The same depth averaging procedure is formally applied to the fluid flow equations. With the kinematic boundary condition at the interface:

$$w(h_o) = \delta \partial_t \zeta + \varepsilon \delta u_k(h_o) \partial_k \zeta \quad (7)$$

the depth averaged continuity equation for each of two fluid layers with the variable depths $\bar{h}_i(x, y, t)$ is

$$\partial_t \zeta = \partial_j (\bar{h}_i - \varepsilon \zeta) \bar{u}_j, \quad (8)$$

which is accurate to all orders in ε and δ .

The depth averaged horizontal momentum equations for each of the fluid layers are

$$\begin{aligned} \partial_t \bar{u}_j + \varepsilon \bar{u}_{ko} \partial_k \bar{u}_{jo} + O(\varepsilon \delta) = \\ = -\varepsilon^{-1} \partial_j P - \partial_j \zeta + \delta^2 \frac{\bar{h}_i^2}{3} \partial_{ijk} \bar{u}_{ko} + O(\varepsilon \delta^2) - \mu \bar{u}_j + E \bar{f}_j \end{aligned} \quad (9)$$

where the continuity of the pressure at the interface is satisfied by introducing $P(x, y, t)$ - the pressure at the interface common to both layers. The linear friction law is introduced in (9):

$$-\mu \bar{u}_j = \frac{1}{\bar{h}_i - \bar{h}_o} \text{Re}^{-1} \varepsilon \delta^{-2} \partial_z u_j \Big|_{\frac{\bar{h}_i}{\bar{h}_o}}, \quad (10)$$

which was used previously for shallow water identifications both for sea tide simulations⁷ and aluminium electrolysis problems⁸. The appropriate boundary conditions to solve the equations (8),(9) are zero normal velocity at the side walls:

$$u_n = 0. \quad (11)$$

The momentum (9) and continuity (8) equations for the two fluid layers can be combined in one nonlinear wave equation for the interface:

$$\begin{aligned} \left\langle \frac{\rho}{h} \right\rangle \partial_{tt} \zeta - \delta^2 \frac{1}{3} \langle \rho \bar{h} \rangle \partial_{ttt} \zeta + \left\langle \frac{\mu \rho}{h} \right\rangle \partial_t \zeta + \langle \rho \rangle \partial_{jj} \zeta = \\ \left\langle \rho E \partial_j \bar{f}_j \right\rangle - \varepsilon \left\langle \frac{\rho}{h} \partial_{ij} (\zeta u_{jo}) + \rho \partial_j (u_{ko} \partial_k u_{jo}) + \frac{\mu \rho}{h} \partial_j (\zeta u_{jo}) \right\rangle \end{aligned} \quad (12)$$

where $\langle F \rangle = F_1 - F_2$ denotes a difference of quantity in the two layers. Note, that $\bar{u}_0 = u_0$ according to (4), and the equation (12) contains only the leading order velocities which can be determined from linear fluid flow equations. For this purpose these velocities are expressed as:

$$\begin{aligned} u_{xo} &= -\partial_y \Psi + \partial_x \chi \\ u_{yo} &= \partial_x \Psi + \partial_y \chi, \end{aligned} \quad (13)$$

then

$$\begin{aligned} (\text{curl } \mathbf{u}_o)_z &= \partial_{kk} \Psi \\ \text{div}_2 \mathbf{u}_o &= \partial_{kk} \chi, \end{aligned}$$

and we need to solve the following additional linear equations:
 curl of linear momentum equation (in layer i):

$$\partial_{kk}\Psi = -\mu_i \partial_{kk}\Psi + E_i \text{curl}_z \bar{\mathbf{F}}_i \quad (14)$$

and linear continuity equation:

$$\partial_t \zeta = \bar{h}_i \partial_{kk} \chi. \quad (15)$$

The coupled electromagnetic force is expressed similar as in Ref.² The horizontal electromagnetic force appearing in (12) and (14) is given by

$$\bar{\mathbf{F}}_j = -\frac{\sigma_1}{\sigma_2} \epsilon \delta \nabla \Phi \times \mathbf{B}_{oz} = O(1). \quad (16)$$

The equation for the electric potential $\Phi(x,y,t)$ in the aluminium is²

$$s^{-1} \bar{h}_1 \bar{h}_2 \partial_{kk} \Phi + \Phi - \frac{\bar{h}_1}{\bar{h}_3 - \bar{h}_2} \Phi = j_o \zeta, \quad (17)$$

where $s = \frac{\sigma_2}{\sigma_1} \delta^{-2} = O(1)$, electrical conductivities for liquid aluminium being $\sigma_j = 3.3 \cdot 10^6$ and for liquid electrolyte - $\sigma_2 = 2 \cdot 10^2 \Omega^{-1} \text{ m}^{-1}$. The nonconducting side walls of the electrolysis cell mean the boundary condition:

$$\partial_n \Phi = 0. \quad (18)$$

Solution and Results

The coupled equations of the problem (11)-(18) are put in a weak form by integrating against sufficiently regular functions over the cell and accounting for the boundary conditions. The solutions of the problem can be expressed in the form:

$$\zeta(x, y, t) = \sum_{k,j} e^{\omega_j t} \zeta_{kj} \cos k_x x \cos k_y y, \quad (19)$$

where the wave vector $\mathbf{k} = (\frac{\pi m}{L_x}, \frac{\pi n}{L_y})$ $m, n = 0, 1, 2, \dots$; and similar expressions for other unknowns Ψ, χ, Φ .

The problem is homogenous what results in a nonlinear eigenvalue problem for ω_j . For linear problem, $\epsilon = 0$, it is possible to solve the homogenous problem for the eigenvalues and eigenvectors. Then the evolution problem with initial conditions is solved by double summing up all eigenvectors for all the respective eigenvalues. The same method can be applied to the nonlinear problem, when $\epsilon \neq 0$, performing a linearization over a small time interval Δt and computing the linear velocity components from the previous time step. The end of previous time step gives new initial conditions for the new linearized problem. At

the each time step the computed eigenvectors need to be normalized according to these initial conditions. Accurate routines for these linear algebra tasks are supplied in the LAPACK program package. Typical runs were made with 16*16 modes in the horizontal directions, and the time steps up to 2.5 seconds were accessible.

Significant efforts were done to validate the problem final formulation and the numerical simulation program against the previously published results. The simple analytical case for two mode, (0,1) and (1,0), interaction, when

$$\zeta = \zeta_{1,0} \cos \frac{\pi}{L_x} x + \zeta_{0,1} \cos \frac{\pi}{L_y} y, \quad (20)$$

permits to recover the previous linear theory² ($\epsilon = 0, \delta = 0, \mu = 0$) result for the critical uniform vertical magnetic field magnitude:

$$B_{0cr} = \frac{(\rho_1 - \rho_2)g\pi^4 H^2}{16I} \left| \frac{L_x}{L_y} - \frac{L_y}{L_x} \right|.$$

In particular, the square cell case $L_x = L_y$ is always unstable if the friction coefficient $\mu = 0$. This is the simplest case of the so called rotating wave instability. The present theory permits to show that the instability holds even for the dispersive case with finite $\delta \neq 0$. However, for

$$\mu \geq \frac{8IB_o}{(\rho_1 - \rho_2)g\pi^4 H^2}$$

this simplest case becomes stable.

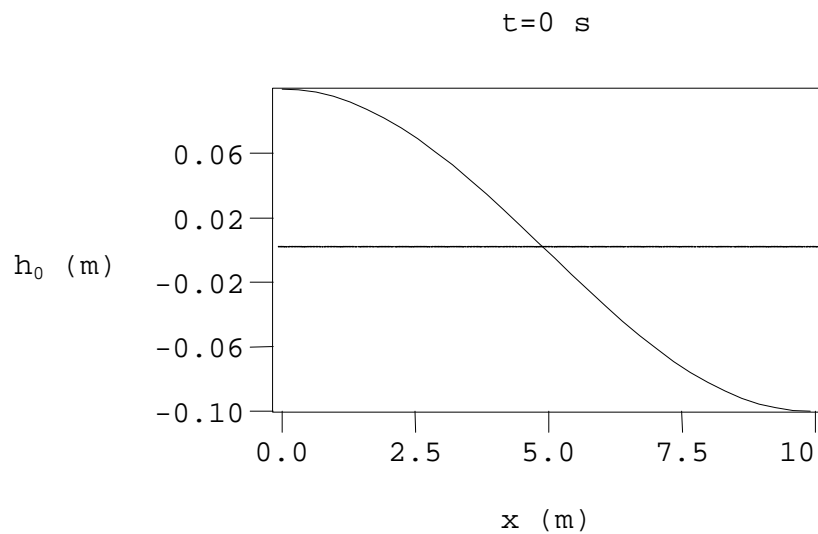


Fig. 2 Wave profile at t=0.

t=920 s, M=4

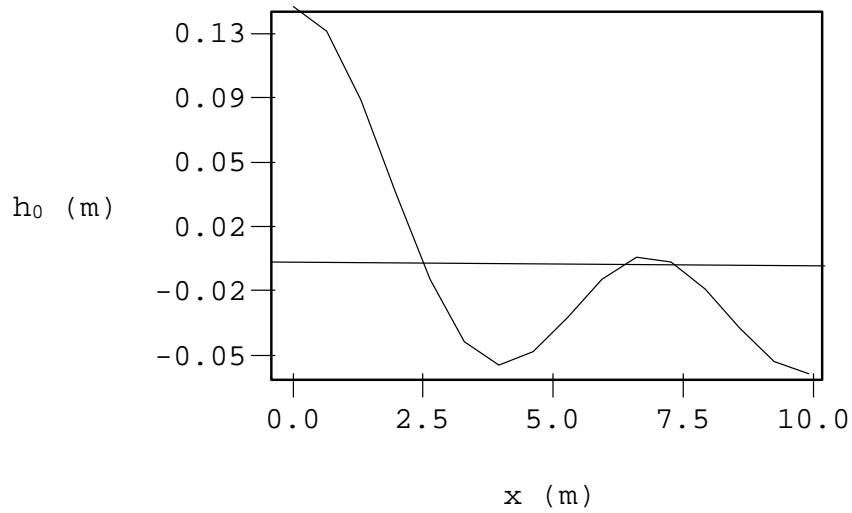


Fig. 3 Wave profile at $t = 920$ s, $m = 4$.

Another checks were made against the analytical results⁶ for a pure hydrodynamic standing wave in the weakly nonlinear case. If started from a (1,0) one dimensional gravity wave (Fig.2), the evolving wave is losing its cosine profile in space and time, and finally the profile maximum elevation is not equal the minimum depression (Fig.3). The present simulation profile is the same as the analytical result⁶ for $m=4$.

t=920 s, M=8

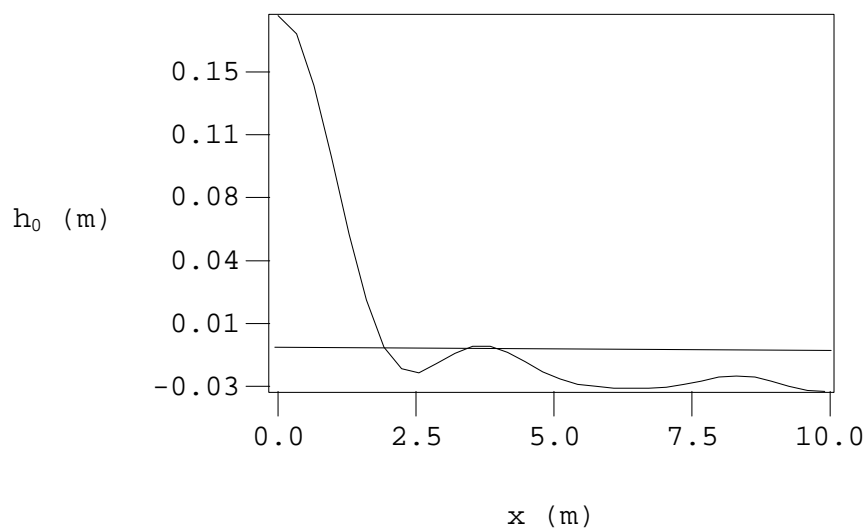


Fig. 4 Wave profile at $t = 920$ s, $m = 8$.

The present numerical method permits to increase number of modes, thus Fig.4 shows the profile for $m=8$ which is different from the 4 mode case. The result was checked increasing still more the number of modes, the Fig.5 shows computed profile for $m=64$, which is the same as for $m=8$.

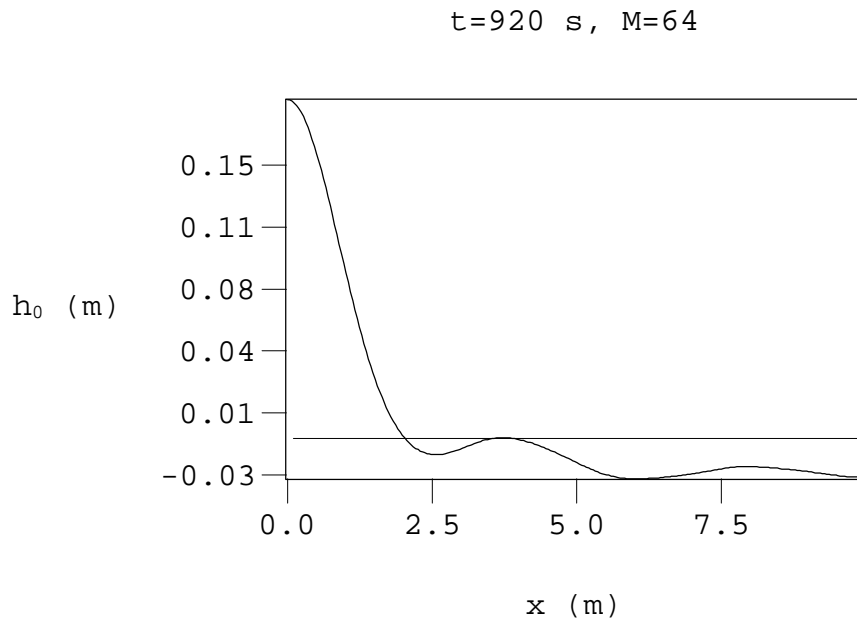
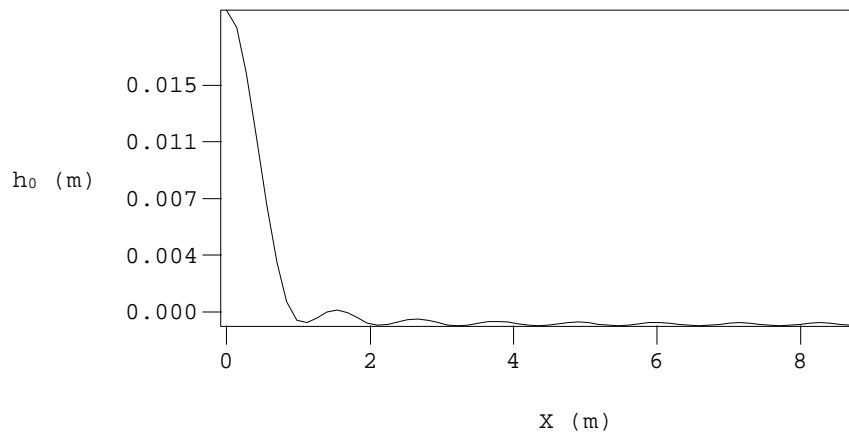
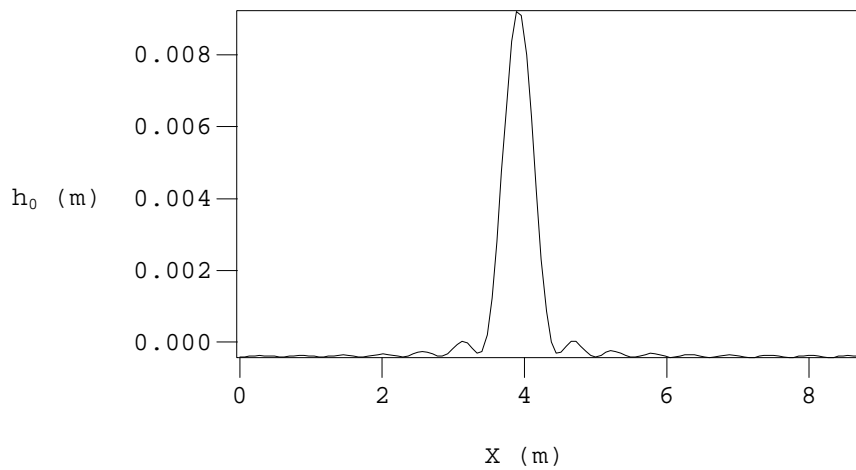


Fig. 5 Wave profile at $t = 920 \text{ s}, m = 64$.

A hydrodynamic solitary wave was attempted to simulate numerically starting with a step like perturbation. It was found that for the considered two fluid particular case the dispersive effects were much stronger expressed than the nonlinear. Therefore a single fluid case ($\rho_2=0$) was considered for the following test exercise. The Fig. 6 shows the initial pulse resulting after Fourier

Initial pulse $T=0$, $M=16$ **Fig. 6 Wave profile, initial pulse.**

representation was applied to the step like perturbation. This pulse travels the channel length ($L=10$ m) many times with reflections, the typical period being approximately 30 seconds. Fig. 7 shows the profile at 1200 seconds.

Linear pulse: $\varepsilon=0$, $\delta=0$ $T=1200$ s**Fig. 7 Wave profile, linear pulse.**

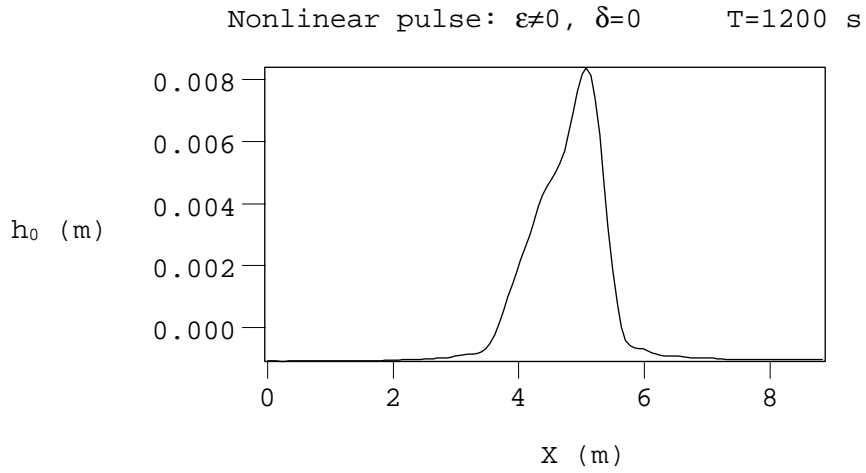


Fig. 8 Wave profile, nonlinear pulse.

The nonlinear wave without dispersion ($\delta=0$) shows a steep front profile (Fig.8). Yet pure dispersive pulse exhibits a typical dispersive tail shown in Fig.9. Finally the dispersive nonlinear wave is shown in Fig. 10.

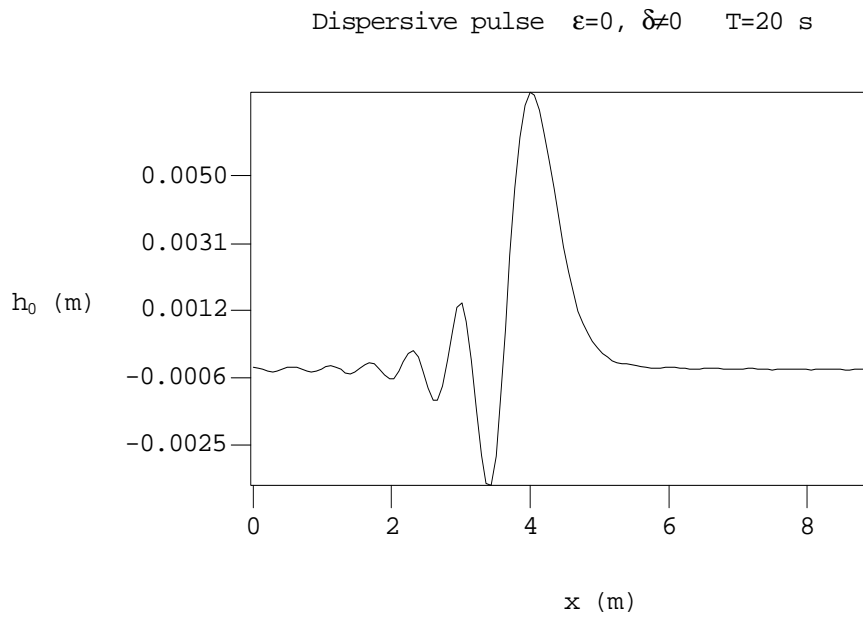


Fig. 9 Wave profile, dispersive pulse.

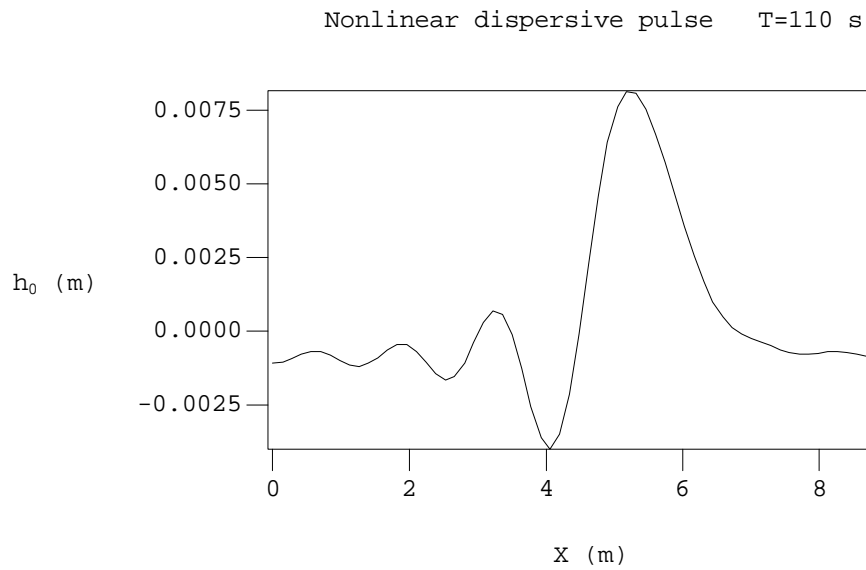


Fig. 10 Wave profile, nonlinear dispersive pulse.

In the case of applied uniform vertical magnetic field the numerically simulated solitary wave initially starts to bounce from one side to other (Fig.11), and at longer times establishes a quasistationary pattern which is totally different from the nonmagnetic case. For a typical electrolysis cell situation this is shown in Fig.12. It is remarkable, that this result is not dependent on the initial conditions. Starting from a depression perturbation, the initial traveling wave is shown in Fig. 13, yet the long time behavior, shown in Fig. 14, is quite similar to the previous case (compare Fig. 12). However, we need to note that the particular wave patterns evolving from the electromagnetic interaction depend on the cell geometrical and material parameters, and on the magnetic field distribution which is affected by the current supply and removal at the cell.

Non-linear waves with electromagnetic interaction

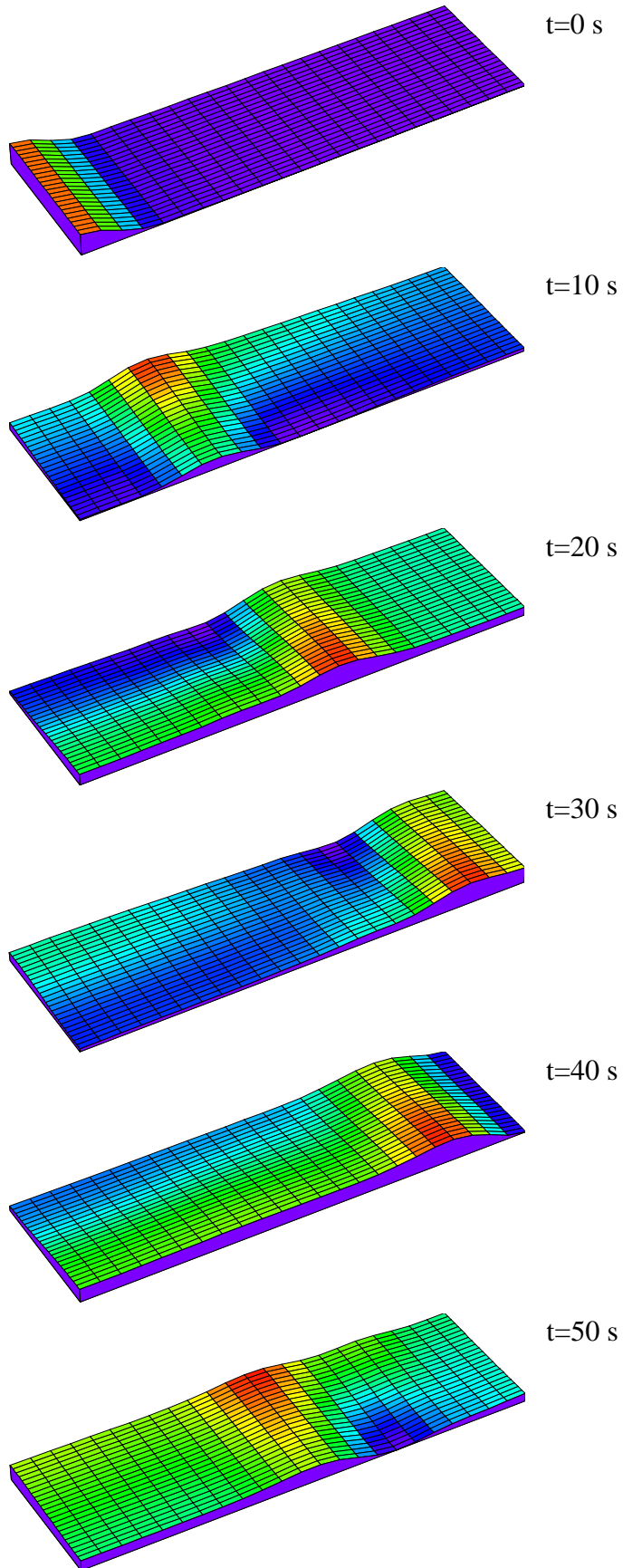


Fig. 11 Initial propagation of the step perturbation
 $L_x=9.8$ m, $L_y=3.2$ m, $B_z=0.003$ T, $I=160000$ A.

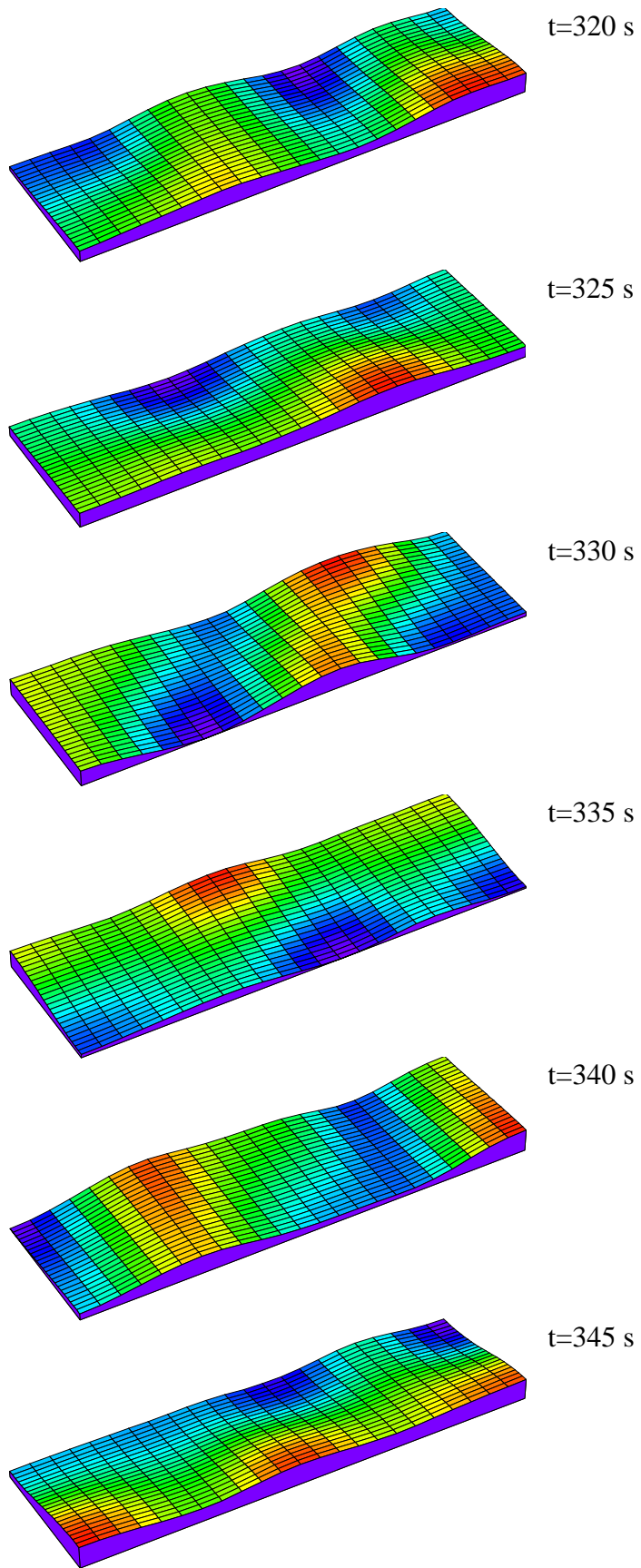


Fig. 12 Established oscillations (from initial step perturbation)
Lx=9.8 m, Ly=3.2 m, Bz=0.003 T, I=160000 A.

Non-linear waves with electromagnetic interaction

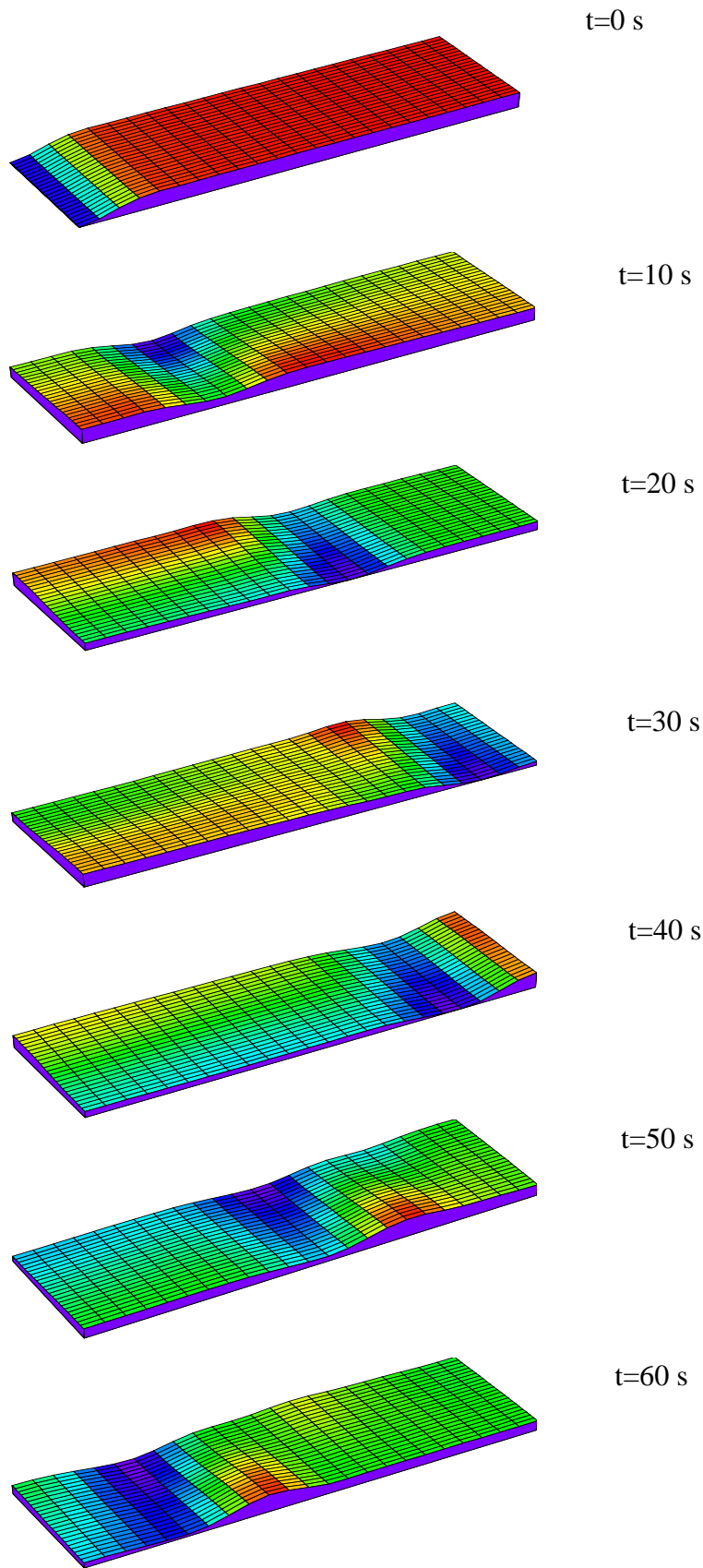


Fig. 13 Initial propagation of the depression at two fluid interface
 $L_x=9.8$ m, $L_y=3.2$ m, $B_z=0.003$ T, $I=160000$ A.

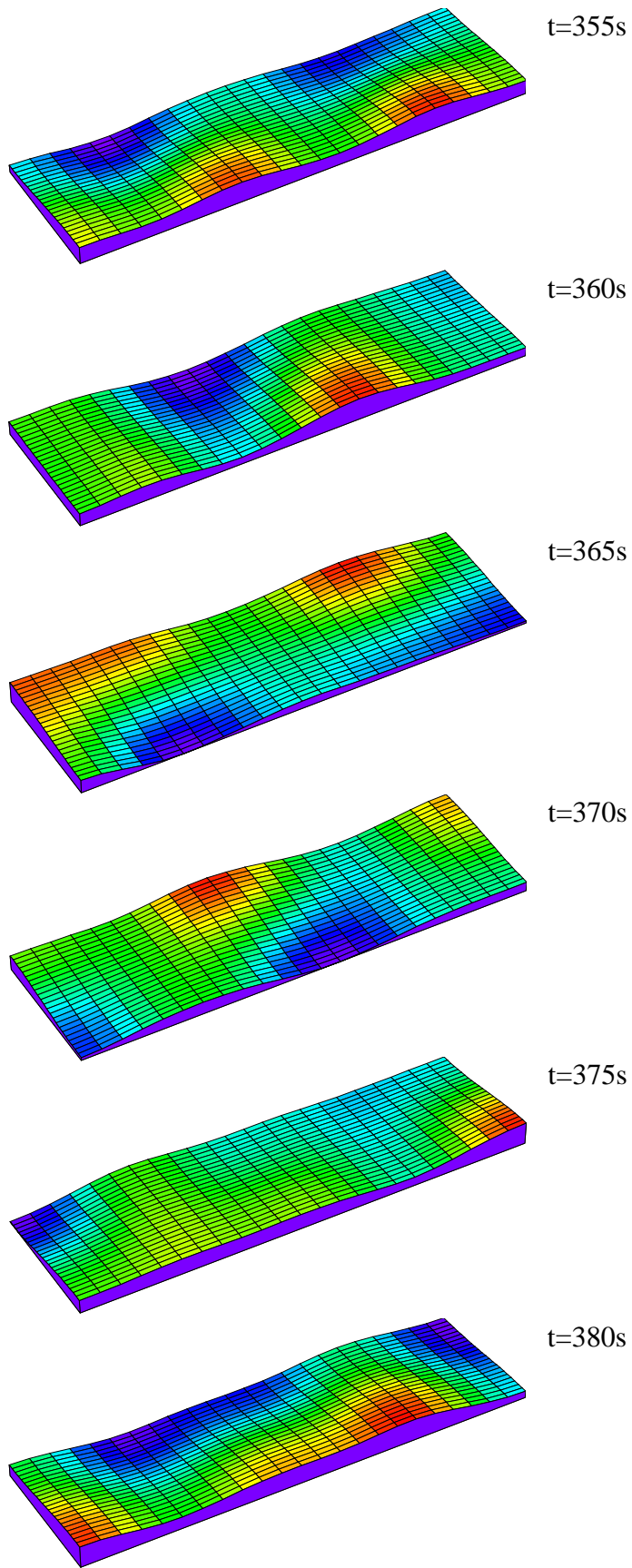


Fig. 14 Established oscillations (from initial depression perturbation)
 $L_x=9.8$ m, $L_y=3.2$ m, $B_z=0.003$ T, $I=160000$ A.

Acknowledgment. The research described in this publication was made possible in part by Grant N LBF000 8 from the International Science Foundation.

References

- ¹ Urata, N., Mori, K., Ikeuchi, H., "Behavior of bath and molten metal in aluminium electrolytic cell," *Keikin-zoku*, Vol.26, No 11, 1976, pp.573-600.
- ² Bojarevics, V. and Romerio M.V., "Long waves instability of liquid metal-electrolyte interface in aluminium electrolysis cells: a generalization of Sele's criterion," *Eur. J. Mech., B/Fluids*, Vol.13, No 1, 1994, pp.33-56.
- ³ Hofman, M., "Nonlinear wave on the free surface of an electrically conducting liquids," *Wave Motion*, Vol.5, April 1983, pp.115-124.
- ⁴ Oshima, S., Yamane, R., "Nonlinear wave of liquid metals under a transverse magnetic field," *Liquid Metal Flows: Magnetohydrodynamics and Applications. Beer-Sheva 5th Internat. Seminar*, edited by H. Branover, M. Mond, Y.Unger, AIAA, 1987, pp.100-118.
- ⁵ Renouard, D.P., Tomasson, G.G., Melville, W.K., "An experimental and numerical study of nonlinear internal waves," *Physics of Fluids, A*, Vol. 5, No 6, 1993, pp.1401-1411.
- ⁶ Tadjbakhsh, I. and Keller, J.B., "Standing surface waves of finite amplitude," *Journal of Fluid Mechanics*, Vol. 8, 1960, pp.442-451.
- ⁷ Heemink, A.W., "Two dimensional shallow water flow identification," *Applied Mathematical Modelling*, Vol. 12, 1988, pp.109-118.
- ⁸ Moreau, R. and Ewans, J.W., "An analysis of the hydrodynamics of aluminium reduction cells," *Journal of Electrochemical Society*, Vol. 131, No 10, pp.2251-2259.